Scientific Research Publishing

Journal of Biosciences and Medicines, 2025, 13(9), 88-104
https://www.scirp.org/journal/jbm
ISSN Online: 2327-509X
ISSN Print: 2327-5081

Preparation and Evaluation of Paclitaxel-Loaded Albumin Nanoparticles Containing Thermo-Sensitive Hydrogel

Peixuan Hu[1,2*], Naicong Cai[3*], Naseer Sintali Dahiru[3*], Hua Wu[1#]

[1]Department of Nutrition, Nanjing University of Chinese Medicine, Nanjing, China
[2]Nanjing Foreign Language School, Nanjing, China
[3]Department of Pharmaceutics, School of Pharmacy, China Pharmaceutical University, Nanjing, China
Email: #170589@njucm.edu.cn

How to cite this paper: Hu, P.X., Cai, N.C., Dahiru, N.S. and Wu, H. (2025) Preparation and Evaluation of Paclitaxel-Loaded Albumin Nanoparticles Containing Thermo-Sensitive Hydrogel. *Journal of Biosciences and Medicines*, **13**, 88-104.
https://doi.org/10.4236/jbm.2025.139008

Received: July 28, 2025
Accepted: August 30, 2025
Published: September 2, 2025

Abstract

The development of long-acting drug preparations is a crucial strategy for enhancing the safety, efficacy, and patient compliance of clinical treatments for certain diseases. In the field of oncology, the world's first long-acting anti-tumor microsphere formulation (Lupron Depot®) was approved in the United States as early as the 1980s. However, microsphere formulations suffer from drawbacks such as complex manufacturing processes, challenging quality control, and stringent storage requirements. To address these limitations, this study aimed to develop a novel intranasal injectable thermosensitive gel formulation loaded with albumin-bound paclitaxel nanoparticles (BSA-PTX NPs) and characterize it *in vitro*. We first optimized the BSA-PTX NP formulation using single-factor experiments followed by Box-Behnken response surface methodology. The optimized nanoparticles exhibited a particle size range of 95.85 - 181.25 nm, an encapsulation efficiency of 47.67% - 96.73%, and a drug loading capacity ranging from 4.33% to 8.79%. Subsequently, Poloxamer was selected as the gel matrix, and the optimal excipient concentrations were determined. Finally, the influence of BSA-PTX NPs loading on the gel's phase transition temperature was investigated, and drug release studies were conducted. The results demonstrate that the Poloxamer-based thermosensitive gel loaded with BSA-PTX NPs is simple to prepare, exhibits excellent injectability, and possesses a body temperature-responsive phase transition temperature. This formulation represents a promising in-situ forming, long-acting anti-tumor drug delivery system. The optimized thermosensitive hydrogel was composed of 18% Poloxamer 407, 0.1% Poloxamer 188, and 0.5% hyaluronic acid,

*These authors contributed equally to this work.
#Corresponding author.

with a phase transition temperature of 32.1˚C ± 0.1˚C. *In vitro* drug release studies showed that over 80% of paclitaxel was released within 48 h in pH 5.5 buffer, exhibiting a sustained release profile.

Keywords

Long-Acting Intranasal Injectable Formulation, Formulation Optimization, Poloxamer, Phase-Transition Temperature, Drug Release

1. Introduction

Paclitaxel, also known as Taxol, taxon, or TM, a member of the taxane family, is one of the most potent, effective, and commercially successful antineoplastic agents for the treatment of advanced and refractory cancers. Paclitaxel was initially isolated from the bark of the Pacific yew tree, *Taxus brevifolia*, and its crude extract was found to have high activity against mouse tumor cells [1]. Subsequently, the chemical structure of this active ingredient was determined by X-ray analysis and verified to be a highly efficacious and broad-spectrum natural anticancer drug with low toxicity [1]. Paclitaxel is a mitotic inhibitor used in cancer chemotherapy and has been approved to treat other solid tumors [2].

In recent decades, albumin-based nanoparticles have received considerable interest due to their biological origin, biodegradability, lack of toxicity, non-immunogenicity, water solubility, ease of availability, and, more importantly, their ability to accumulate in tumor sites [3]-[5]. Abraxane is a well-known albumin-based nanoparticle of the chemotherapeutic agent paclitaxel with a mean particle size of 130 nm, approved by the FDA in 2005 to treat metastatic breast cancers [6] [7]. Albumin nanoparticles can be prepared by four main effective methods, namely desolvation, emulsification, thermal gelation, and, recently, nano spray drying. Nab-technology and self-assembly techniques have also been used [5]. When compared to other proteins, albumin nanoparticles have attracted considerable interest as drug carriers because they have several unique features [3]: they are non-toxic and well tolerated by the immune system; exhibit a high reversible binding capacity to hydrophobic drugs [4]; and have a favorable pharmacokinetic profile owing to their long half-life in the blood system (19 days) [8].

Naturally derived polymers such as collagen, chitosan, Matrigel, and agarose can be used as, or modified to be, thermosensitive hydrogels. Their excellent biocompatibility makes them preferred candidates for drug carriers. However, they are less versatile for modification compared with their synthetic counterparts. Poloxamer molecules self-associate due to their surfactant properties, forming micelles at a specific concentration known as the critical micelle concentration (CMC). During micelle formation, the PPO groups interact via van der Waals forces to form the core of the hydrophobic micelle, whereas the PEO groups occupy the micelle shell, interacting with water molecules via hydrogen bonds [9].

Temperature increase favors interactions between PPO groups and polymer desolvation, thus enhancing micelle formation at lower polymer concentrations [9]. Upon further heating of the micellar aqueous solution, poloxamer micelles aggregate at a specific temperature, and the system fluidity decreases abruptly, leading to gel formation. This process is reversible because cooling converts the gel back to its original sol state [10]. This study, therefore, aimed to develop an albumin-based nanoparticle loaded with PTX, formulated into a thermosensitive gel. This thermosensitive gel is intended for intranasal administration, with a target phase transition temperature close to the nasal cavity temperature (32˚C).

2. Methods

2.1. Materials

Bovine serum albumin (BSA) was purchased from Sigma-Aldrich (USA). Paclitaxel was obtained from Wuxi Taxus Pharmaceutical Co. Ltd. Acetonitrile was purchased from Tedia Company, Inc. 1-Ethyl-3-(3-dimethylaminopropyl) carbodiimide hydrochloride (EDC·HCl) was obtained from Shanghai Medpep Co. Ltd. Hyaluronic acid and pepsin were purchased from Shanghai Aladdin Biochemical Technology Co., Ltd. Poloxamer 407 (P407) and Poloxamer 188 (P188) were obtained from BASF. All other chemicals used were of analytical grade.

2.2. Preparation of PTX-Loaded BSA-NPs

PTX-loaded BSA-NPs were prepared using a simple desolvation process for nanoparticles. The required amounts of BSA (12.5, 25.0, 37.5, and 50 mg/mL) were dissolved in 4 mL of purified water and filtered. The solution was stirred using a magnetic stirrer at 1000 rpm, while 4.5 mL of ethanol was added at a flow rate of 1 mL/min with a peristaltic pump and the turbidity of the mixture was observed. Ten mg of PTX was dissolved in 1 mL ethanol and added to the BSA nanoparticles using a peristaltic pump at a flow rate of 1 mL/min. The formulation was stirred continuously at 1000 rpm for 10 min to mix the drug and the nanoparticles. Afterwards, EDC·HCl (2.5 mg in 0.5 mL of water), which acted as a crosslinker, was added at room temperature for 3 h. The resulting solution was collected and purified by high-speed centrifugation at 12,000 rpm at room temperature for 30 min. This process was repeated three times. The nanoparticles were suspended in 4 mL of distilled water twice. Finally, the PTX-loaded BSA nanoparticles were collected and used for the preparation of the thermosensitive gel.

2.3. Optimization of BSA-PTX-NP Formulations

To optimize the nanoparticle formulations, the effect of various factors (BSA concentration, BSA/drug ratios, BSA/EDC ratios, ethanol flow rate, and pH) on the response (particle size, polydispersity index (PDI), entrapment efficiency, and drug loading) was determined. To further optimize the formulations, Design Expert® 8.0 software was used to check the Box-Behnken surface response of the formulations. The Box-Behnken models are defined based on the factors and levels

set. The formulations were obtained with 17 designed experiments and were tested three times to confirm formulation reproducibility.

2.4. Determination of Particle Size

The particle size distribution and zeta potential of BSA-PTX NPs were determined by dynamic light scattering (DLS) using a particle size analyzer (Nano Brook Series (Brookhaven Instruments)). The particle size was evaluated by intensity measurement. The particle size was measured at 25˚C with a scattering angle of 90˚. The zeta potential was measured at 25˚C. Both particle size and zeta potential measurements were performed in triplicate.

2.5. Drug Entrapment Efficiency (EE) and Drug Loading Efficiency (DL)

The encapsulated drug was determined by HPLC. In brief, 0.1 mL BSA-PTX NPs solution was added to 1 mL of 1% pepsin solution and incubated at 37˚C in a water bath for 30 min. Pepsin was added to degrade the albumin matrix of BSA-PTX NPs, thereby releasing the encapsulated paclitaxel. Then, 5 mL of acetonitrile was added and centrifuged for 10 min at 12,000 rpm at 4˚C. 0.1 mL of the separated supernatant was then added to 0.9 mL of mobile phase for HPLC analysis.

$$\mathrm{EE}\% = \frac{W_1}{W_0} \times 100\% \tag{1}$$

$$\mathrm{DL}\% = \frac{W_1}{\mathrm{PTX} + \mathrm{BSA}} \times 100\% \tag{2}$$

where EE (Entrapment Efficiency), DL (Drug Loading), W_1 (Actual amount of PTX in nanoparticles), W_0 (Nominal amount of PTX in nanoparticles).

2.6. Formulation of Thermosensitive Hydrogel

The cold method was adopted from previous work to prepare the thermosensitive gel [11] [12]. 5% hyaluronic acid solution was prepared by dissolving an appropriate amount in 4 mL purified water chilled to 4˚C. Subsequently, the weighed portions of P407 and P188 were slowly added and stirred continuously for 30 minutes. The mixture was then incubated at 4˚C for 12-24 h to completely hydrate and dissolve the P407 and P188.

2.7. Optimization of Thermosensitive Hydrogel

Various portions of P407 and P188 between 16.0% - 24.0% and 0.1% - 1.5%, respectively, were prepared into gels using 0.5% hyaluronic acid. The gelation temperatures and viscosities of the various gels were then evaluated.

2.8. Determination of Gelation Temperature

The gelation temperature of the formulated products was determined by the tube inversion method as reported previously [12] [13]. 4 mL of the hydrogel was transferred into a thermostat-controlled electric water bath set at an initial temperature

of 20˚C, with a gradual increment at a rate of 0.5˚C/min. The temperature at which the meniscus of the hydrogel did not move when the vial was tilted to a 90˚ angle was identified as the gelation temperature. This test was performed in triplicate.

2.9. Determination of Viscosity

The viscosity was determined using a Brookfield DV2 Ultra-type rotor viscometer with rotor SC 18, set at 10 rpm, and at 25˚C for 2 min. The viscosities of the respective solutions were determined and compared. This test was performed in triplicate.

2.10. Preparation of BSA-PTX NPs Thermosensitive Gel

The 2.5 mg/mL PTX-BSA NPs formulation was selected based on optimization results (Section 3.1), which showed that this formulation had a suitable particle size (176.94 ± 5.08 nm), low PDI (0.107 ± 0.067), and moderate entrapment efficiency (50.78%), ensuring good compatibility with the poloxamer gel matrix and efficient drug release. To prepare a 2.5 mg/mL PTX-BSA nanoparticle suspension, hyaluronic acid and poloxamer-407 were added to attain concentrations of 0.5% w/v and 18% w/v, respectively. The sample was then mixed for 30 minutes and later stored at 4˚C for approximately 12 - 24 h.

2.11. Determination of the Gelation Temperature for BSA-PTX NPs Thermosensitive Gel

The gelation temperature of the formulated products was determined by the tube inversion method [12] [13]. 4 mL of the hydrogel was transferred into a thermostat-controlled electric water bath set to 20˚C. The gel was allowed to acclimatize for 5 min, followed by a gradual increase in temperature set at a rate of 0.5˚C/min. The temperature at which the meniscus of the hydrogel did not move when the vial was tilted to a 90˚ angle was identified as the gelation temperature. This test was performed in triplicate.

2.12. *In Vitro* Drug Release

The *in vitro* release of PTX within hydrogel BSA-PTX-NPs was studied. 5 g of cold BSA-PTX NPs hydrogel was transferred into a centrifuge test tube and placed in a water bath set at 33˚C. The gel was allowed to acclimatize for 10 min. 10 mL of phosphate buffer (pH = 5.5) was layered over the hydrogel and incubated for 48 h. At various time intervals (2 h, 4 h, 6 h, 8 h, 12 h, 24 h, and 48 h), 1 mL of the buffer was taken with an equal volume of fresh buffer replaced. Each sample was filtered and analyzed with the HPLC. This test was repeated with phosphate buffer (pH = 7.4) under the same conditions.

3. Results and Discussion

3.1. Optimization of the Formulations

To optimize the formulation, various factors that affect the preparation of BSA-

PTX NPs were evaluated using the desolvation process. The particle sizes, PDIs, EE, and DL can be observed in Table 1. The suitable ideal method of preparation was determined using a single-factor experiment with the Box-Behnken response surface design, and the best formulation process was observed.

Table 1. Optimization of formulations by analyzing the various factors that affect particle size, PDI, EE, and DL.

	BSA (mg)	PTX (mg)	EDC (mg)	Ethanol flow rate (mL/min)	pH	Particle size (nm)	PDI	EE (%)	DL (%)
BSA Concentration	50	5	1.25	1.0	-	2001.72 ± 439.24	2.082 ± 0.529	43.63	3.97
	100	10	2.5	1.0	-	176.94 ± 5.08	0.107 ± 0.067	50.78	4.62
	150	15	3.75	1.0	-	1124.91 ± 106.53	0.179 ± 0.100	92.31	8.39
	200	20	5	1.0	-	876.07 ± 93.23	0.482 ± 0.344	92.86	8.44
BSA:PTX ratio	100	20	2.5	1.0	-	267.74 ± 14.30	0.262 ± 0.029	40.53	3.68
	100	10	2.5	1.0	-	214.55 ± 1.05	0.152 ± 0.022	36.64	3.33
	100	6.25	2.5	1.0	-	1411.02 ± 264.69	0.184 ± 0.155	87.14	7.92
	100	5	2.5	1.0	-	648.82 ± 20.97	0.127 ± 0.089	75.00	6.82
Ethanol flow rate	100	10	2.5	0.5	-	1706.34 ± 203.79	1.285 ± 0.553	79.49	7.23
	100	10	2.5	1.0	-	499.70 ± 36.16	0.175 ± 0.038	85.11	7.74
	100	10	2.5	1.5	-	1190.73 ± 130.75	1.126 ± 0.782	97.78	8.89
	100	10	2.5	2.0	-	692.69 ± 82.10	0.384 ± 0.199	91.53	8.32
pH ratio	100	10	2.5	1.0	6	1694.67 ± 570.60	1.973 ± 1.652	83.33	7.58
	100	10	2.5	1.0	7	151.45 ± 4.00	0.244 ± 0.027	88.34	8.03
	100	10	2.5	1.0	8	177.36 ± 2.52	0.132 ± 0.003	91.10	8.28
	100	10	2.5	1.0	9	195.14 ± 6.45	0.264 ± 0.038	36.65	3.33

Different BSA concentrations (12.5, 25.0, 37.5, and 50 mg/mL) were prepared and evaluated to identify the optimal concentration for synthesizing nanoparticles with acceptable sizes. The influence of BSA concentration on the nanoparticles' diameter is shown in (Table 1). 25 mg/mL of BSA was observed as the required concentration for optimum nanoparticle size of 176.94 ± 5.08 nm. All other concentrations produced nanoparticles with unfavorable sizes. In previous work, Langer *et al.* [14] demonstrated that the concentration range of 25 - 100 mg/mL for HSA profoundly influences the particle diameter. Similarly, Galisteo-González and Molina-Bolívar [15], synthesized albumin nanoparticles within size ranges of 100 - 120 nm with BSA concentration in the range of 15 - 50 mg/mL. These results demonstrate the effect of concentration on nanoparticle size.

The determination of the effects of pH on the protein solution in the preparation of albumin nanoparticles was investigated. BSA was dissolved in 10 mM sodium chloride and 10 mM phosphate buffer, with a pH of 7.4. Ethanol was then added dropwise to the prepared mixture at a constant flow rate. Surprisingly, the particle size of the formulations synthesized at pH 6 was larger than 300 nm. Var-

ious buffers (phosphate buffers at pH 7, 8 and borate buffers at pH 8, 9, all at 20 mM and 50 mM) were further tested. Based on the observed results, nanoparticles prepared in the buffer solutions at the optimal pH 7 produced smaller nanoparticle sizes. According to Langer *et al.* [14] salts and buffers are not suitable for the production of BSA nanoparticles. However, Jun *et al.* [16], Galisteo-González and Molina-Bolívar [15], and Taheri *et al.* [17] prepared albumin nanoparticles successfully in the presence of 10 mM NaCl and phosphate buffer.

Our results have shown that with the addition of ethanol at a flow rate of 1.0 ml/min, smaller particle sizes were produced, while a flow rate of 0.5 ml/min produced the highest particle size and PDI (**Table 1**). The addition of a desolvation agent determines the rate and degree of supersaturation and therefore strongly influences the nucleation rate and particle-growth kinetics. When the rate of addition of the desolvation agent increases, the nucleation rate increases, resulting in the formation of larger particles. Moreover, the rate of addition of desolvation agents could change the growth rate of each nucleus. The particle growth rate reflects the mass transfer of protein molecules from the solution phase to the particle surface, and this transfer rate may then depend on how quickly ethanol was added to the protein solution. Similar results have been reported by Kreuter *et al.* in the preparation of gelatin nanoparticles [18]. In their study, the authors found that an increase in the addition of ethanol increased the particle size. In contrast, Kakran *et al.* have reported that an increase in the addition of desolvation agents to curcumin solution reduced the particle size [19]. Some other authors have reported that the rate of addition of desolvation agent has no significant influence on the size of particles but does have an effect on PDI [20].

The drug ratio in the drug formulation and ultimate delivery to the site of action should not be ignored. With any drug, it is possible to alter its bioavailability considerably by formulation modification. An even larger variation between a good formulation and a bad formulation has been observed with some drugs. Based on the observed results, nanoparticles prepared based on drug ratios tend to influence the particle size.

The statistical experimental Box-Behnken response surface design of BSA-PTX NPs was determined with the factors: BSA concentration (*A*), ethanol flow rate (*B*), pH (*C*), and with responses including particle size, PDI, and drug entrapment efficiency (results are shown in **Table 2**).

For regression analysis, Design Expert 8.0 was used, and the quadratic multiple regression model was obtained as follows:

$$\begin{aligned}\text{Particle size} = {} & 102.79 - 23.68A - 5.16B + 5.67C + 39.83AB - 17.50AC \\ & + 23.36BC + 37.30A^2 + 36.17B^2 - 1.49C^2 \qquad (3)\end{aligned}$$

$$\left(R^2 = 0.8366\right)$$

$$\begin{aligned}\text{PDI} = {} & 0.14 - 6.500\text{E}{-}003A - 4.500\text{E}{-}003B + 1.000\text{E}{-}003C + 0.010AB \\ & + 0.013AC + 5.250\text{E}{-}003BC + 4.475\text{E}{-}003A^2 + 0.044B^2 + 0.048C^2 \qquad (4)\end{aligned}$$

$$\left(R^2 = 0.8426\right)$$

Table 2. Optimization of the PTX-BSA NP formulation using box-Behnken design.

Run	Factor 1 *A*: BSA concentration (mg/ml)	Factor 2 *B*: Ethanol Flow Rate (ml/min)	Factor 3 *C*: pH	Response 1 Particle size (nm)	Response 2 PDI	Response 3 EE (%)
1	100	1.00	8	100.31	0.143	92.41
2	100	0.50	7	160.85	0.238	83.34
3	100	1.00	8	108.79	0.140	82.19
4	100	1.00	8	98.65	0.128	96.73
5	80	0.50	8	181.25	0.228	74.52
6	100	1.50	7	118.06	0.215	92.54
7	100	0.50	9	110.15	0.236	95.89
8	120	0.50	8	95.85	0.152	83.63
9	120	1.00	9	139.94	0.217	80.03
10	100	1.50	9	160.80	0.234	89.45
11	100	1.00	8	104.18	0.146	92.19
12	80	1.00	7	102.26	0.192	96.46
13	80	1.50	8	157.02	0.202	47.67
14	80	1.00	9	163.92	0.161	90.18
15	120	1.50	8	150.93	0.167	90.62
16	120	1.00	7	148.26	0.195	79.25
17	100	1.00	8	102.00	0.137	89.26

$$\begin{aligned} \mathrm{DL} &= 8.23 + 0.28A - 0.20B + 0.046C + 0.77AB + 0.16AC \\ &\quad - 0.35BC - 0.92A^2 - 0.57B^2 + 0.55C^2 \\ &\left(R^2 = 0.5499\right) \end{aligned} \tag{5}$$

From the above models, significant differences were tested. The ANOVA results showed that the model's values for the formulations in Table 2 all had $P < 0.05$, and the variables—BSA concentration (mg/mL) (*A*), ethanol flow rate (mL/min) (*B*), and pH of the nanoparticle formulation (*C*)—all had a significant effect on the response of BSA-PTX NPs. The quadratic equation was used for the particle size, PDI, and entrapment efficiency of the nanoparticles, which all showed significant effects except the entrapment efficiency. The correlation coefficients (R^2) of particle size, PDI, and entrapment efficiency were 0.8366, 0.8426, and 0.5499, respectively. There was a correlation among the 17 groups of experiments, the range of particle size was 95.85 to 163.92 nm. In all responses, the factors and interactions of independent variables *A*, *B*, *C*, and particle size were analyzed using a multivariate quadratic equation fitting analysis. The model probability ($P = 0.0410 < 0.05$) and F-value ($F = 3.98$) indicate a significant fit in

Table 3. The factors and interactions of independent variables *A*, *B*, *C*, and PDI were analyzed using a multivariate quadratic equation fitting analysis, with a model probability of P = 0.0366 < 0.05 and F = 4.16, indicating a significant fit in Table 4.

Table 3. Quadratic model of particle size using ANOVA.

Source	Sum of Squares	df	Mean Square	F-value	p-value	significant
Model	11304.15	9	1256.02	3.98	0.0410	significant
A-BSA concentration	603.26	1	603.26	1.91	0.2092	
B-Rate of Ethanol	187.31	1	187.31	0.5938	0.4662	
C-pH	257.42	1	257.42	0.8160	0.3964	
AB	1572.52	1	1572.52	4.98	0.0607	
AC	1224.30	1	1224.30	3.88	0.0895	
BC	2182.76	1	2182.76	6.92	0.0339	
A^2	2094.46	1	2094.46	6.64	0.0366	
B^2	1887.61	1	1887.61	5.98	0.0444	
C^2	768.02	1	768.02	2.43	0.1626	
Residual	2208.19	7	315.46			
Lack of Fit	2146.34	3	715.45	46.27	0.0015	significant
Pure Error	61.85	4	15.46			
Cor Total	13512.34	16				

Table 4. Quadratic model of PDI using ANOVA.

Source	Sum of Squares	df	Mean Square	F-value	p-value	significant
Model	0.0210	9	0.0023	4.16	0.0366	significant
A-BSA concentration	0.0003	1	0.0003	0.6048	0.4622	
B-Rate of Ethanol	0.0002	1	0.0002	0.2899	0.6070	
C-pH	8.000E−06	1	8.000E−06	0.0143	0.9081	
AB	0.0004	1	0.0004	0.7519	0.4146	
AC	0.0007	1	0.0007	1.26	0.2993	
BC	0.0001	1	0.0001	0.1973	0.6703	
A^2	0.0001	1	0.0001	0.1509	0.7093	
B^2	0.0081	1	0.0081	14.57	0.0066	
C^2	0.0097	1	0.0097	17.34	0.0042	
Residual	0.0039	7	0.0006			
Lack of Fit	0.0037	3	0.0012	26.01	0.0044	significant
Pure Error	0.0002	4	0.0000			
Cor Total	0.0249	16				

The effect of independent variables *A*, *B*, and *C* on entrapment efficiency was not significant in the multivariate quadratic equation analysis. The probability (P = 0.5397 > 0.05) and F-value (F = 0.9502) indicate that the relevant results were not significant in Table 5.

Table 5. Quadratic model of entrapment efficiency using ANOVA.

Source	Sum of Squares	df	Mean Square	F-value	p-value	significant
Model	1217.13	9	135.24	0.9502	0.5397	not significant
A-BSA concentration	76.26	1	76.26	0.5358	0.4879	
B-Rate of Ethanol	36.55	1	36.55	0.2568	0.6279	
C-pH	1.96	1	1.96	0.0138	0.9099	
AB	286.29	1	286.29	2.01	0.1991	
AC	12.46	1	12.46	0.0876	0.7759	
BC	61.15	1	61.15	0.4297	0.5331	
A^2	432.54	1	432.54	3.04	0.1248	
B^2	167.67	1	167.67	1.18	0.3137	
C^2	154.60	1	154.60	1.09	0.3320	
Residual	996.27	7	142.32			
Lack of Fit	880.38	3	293.46	10.13	0.0244	significant
Pure Error	115.90	4	28.97			
Cor Total	2213.40	16				

3.2. Surface Morphology

The morphology and size of the developed nanoparticles were investigated using transmission electron microscopy (TEM) (Hitachi, Japan). A drop of the nanoparticulate solution was placed on carbon-coated copper grids. The sample was allowed to dry on the grids, which were then loaded into the instrument and scanned under the microscope to observe the particles. The morphology was found to be spherical (Figure 1).

3.3. Particle Size and Size Distribution

The particle size and size distribution of BSA-PTX NPs prepared in single-factor experiments are depicted in Figure 2. These nanoparticles exhibited particle sizes within the desired range and a narrow size distribution (low PDI).

3.4. Drug Entrapment Efficiency (EE) and Drug Loading Efficiency (DL)

All formulations with different concentrations exhibited good EE and DL (Table 6). The lowest entrapment efficiency and drug loading efficiency were observed in

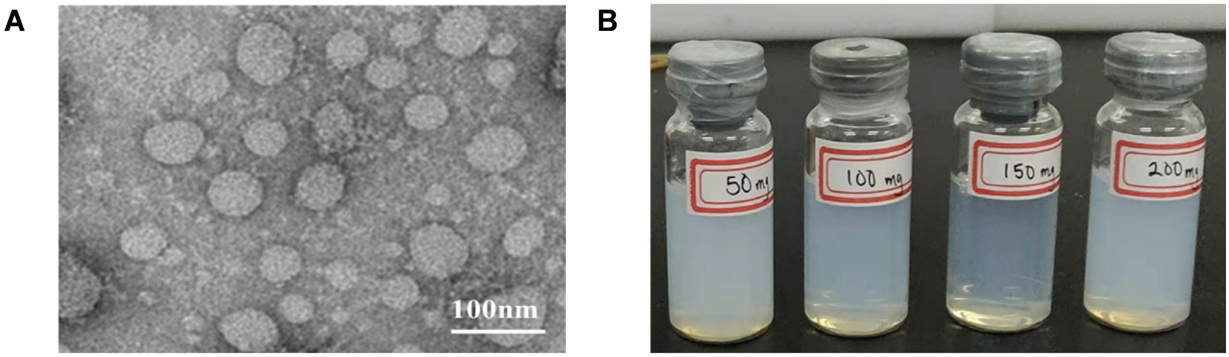

Figure 1. (A) TEM morphology of the BSA-PTX NPs, (B) Different concentrations of BSA-PTX NPs: 12.5 mg/mL, 25.0 mg/mL, 37.5 mg/mL, and 50.0 mg/mL of BSA.

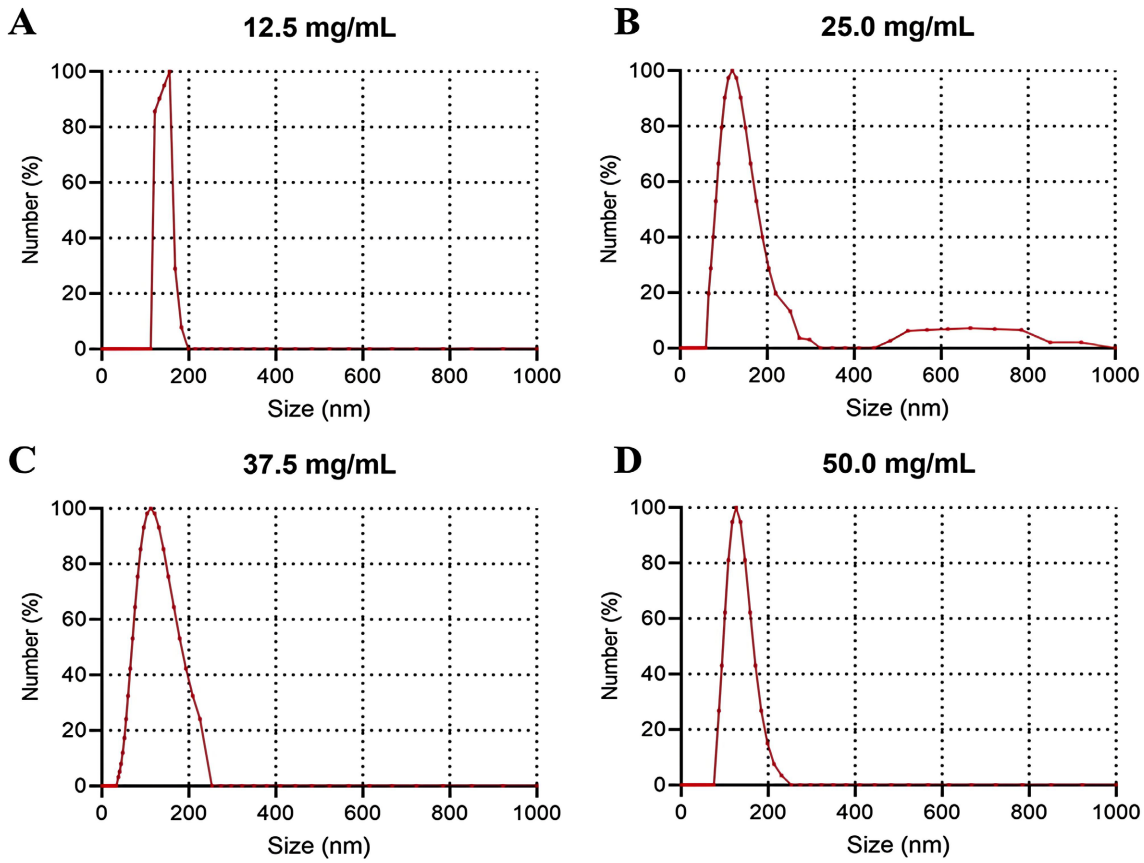

Figure 2. Distribution of particle size with different concentrations of BSA-PTX NPs: (A) 12.5 mg/mL of BSA, (B) 25.0 mg/mL of BSA, (C) 37.5 mg/mL of BSA, (D) 50.0 mg/mL of BSA.

Table 6. Entrapment and loading efficiency.

Concentration of BSA (mg/mL)	Entrapment efficiency (%)	Loading efficiency (%)
12.5	87.50	14.63
25.0	92.43	8.43
37.5	86.14	5.40
50.0	94.87	4.53

preparations with BSA concentrations of 37.5 mg/mL and 50.0 mg/mL, respectively.

3.5. Effect of P407 Formulation on Gelation Temperature

As shown in Figure 3, the sol-gel transition temperature ($T_{sol\text{-}gel}$) of poloxamer formulations decreased as the concentration of P407 increased. The observed decrease in $T_{sol\text{-}gel}$ indicates that stronger gels were formed at high poloxamer concentrations, thus lowering the temperature at which gel formation occurs.

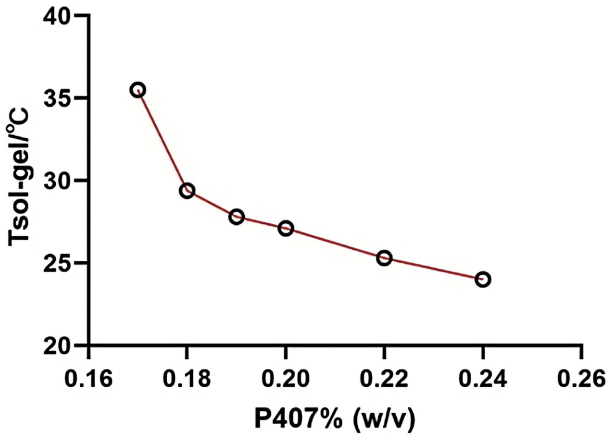

Figure 3. Variation of $T_{sol\text{-}gel}$ dependent on P407 concentration (n = 3).

3.6. Effect of Poloxamer Concentration on Gelation Temperature

The effect of poloxamer on $T_{sol\text{-}gel}$ was studied while combining P407 and P188 in various ratios. Variations in their concentrations and ratios had a significant effect on the $T_{sol\text{-}gel}$. As shown in Table 7, the $T_{sol\text{-}gel}$ values of the various P407/P188 ratios were within 27.2˚C ± 0.1˚C to 41.3˚C ± 0.2˚C. A few of the P407/P188 combinations, such as (18%/0.1%, w/w), (18%/0.15%, w/w), (19%/0.6%, w/w), (20%/1%, w/w), and (20%/1.5%, w/w), had their $T_{sol\text{-}gel}$ values closer to 32˚C. Thus, 32˚C is the target temperature for nasal administration. The higher the concentration of P407, the lower the energy required to form micelles. As observed, increasing the concentration of P407 decreases the $T_{sol\text{-}gel}$, while increasing the concentration of P188 increases the $T_{sol\text{-}gel}$. The ratio of P407/P188 that exhibited the appropriate $T_{sol\text{-}gel}$ was selected for further studies.

3.7. Effect of Bio-Adhesive Agents on Gelation Temperature

As observed in Table 8, the addition of HA to each of the various combinations of P407/P188 affected the $T_{sol\text{-}gel}$. Except for P407/P188 having (18%/0.1%, w/w), all other combinations exhibited lower $T_{sol\text{-}gel}$ values. With the same proportion of P407 and constant HA, elevated $T_{sol\text{-}gel}$ values were observed as the proportion of P188 increased.

3.8. Effect of P407/P188 Ratio on Viscosity

The effect of P407/P188 ratio on viscosity was determined by the rotor viscometer.

Table 7. Effects of P188 and P407 concentrations on the gelation temperature (n = 3).

P407 (%)	P188 (%)	$T_{sol\text{-}gel}$ (˚C)*
18	0.1	32.1 ± 0.1
18	0.15	32.4 ± 0.2
18	0.25	32.7 ± 0.4
18	0.5	33.0 ± 0.1
18	1	36.6 ± 0.2
18	1.5	41.3 ± 0.2
19	0.5	30.0 ± 0.2
19	0.6	32.2 ± 0.2
19	0.7	33.5 ± 0.2
19	1	34.9 ± 0.1
19	1.5	36.9 ± 0.1
20	0.5	29.6 ± 0.3
20	1	31.1 ± 0.1
20	1.5	32.1 ± 0.1
22	0.5	27.2 ± 0.1
22	1	29.1 ± 0.1
22	1.5	30.1 ± 0.1

*Mean ± SD of three replicate measurements.

Table 8. Effects of bio-adhesive material on gelation temperature.

P407 (%)	P188 (%)	HA (%)	$T_{sol\text{-}gel}$ (˚C)*
18	1	0.5	35.6 ± 0.2
18	0.05	0.5	34.4 ± 0.1
18	0.01	0.5	34.6 ± 0.1
19	0.6	0.5	33.3 ± 0.2
19	0.4	0.5	32.7 ± 0.1
19	0.2	0.5	31.7 ± 0.1
20	1	0.5	32.3 ± 0.1
20	1.5	0.5	33.4 ± 0.1
20	0.9	0.5	31.6 ± 0.2
20	0.8	0.5	31.5 ± 0.1

*Mean ± SD of three replicate measurements.

As shown in Table 9, the viscosity increased with the increasing proportion of P407 but decreased with increasing concentration of P188 content in the gel. Sim-

ilarly, in Table 10, the bio-adhesion agent (HA) exhibited varying effects on the viscosity depending on the ratio of P407/P188.

Table 9. Effects of the P407/P188 ratio on viscosity (n = 3).

P407 (%)	P188 (%)	Viscosity (mPa.s)
18	0	59.8 ± 1.9
18	0.1	59.3 ± 0.6
18	0.15	56.9 ± 1.5
19	0	83.2 ± 0.6
19	0.6	75.7 ± 1.4
20	0	114.7 ± 4.5
20	1	100.2 ± 1.5
20	1.5	99.4 ± 2.7

Table 10. Effects of P407/P188 ratio and HA on viscosity (n = 3).

P407 (%)	P188 (%)	HA (%)	Viscosity (mPa.s)
18	0.01	0.5	511.7 ± 14.5
18	0.1	0.5	567.3 ± 13.2
19	0.2	0.5	648.1 ± 16.6
19	0.5	0.5	668.3 ± 6.3
20	0.8	0.5	777.3 ± 49.8
20	1	0.5	743.3 ± 35.3
20	1.5	0.5	784.6 ± 28.5

3.9. Effect of BSA-PTX NPs Hydrogel on the Gelation Temperature

The effect of BSA-PTX NPs hydrogel on gelation temperature is shown in Table 11. The BSA-PTX NPs hydrogel and 18% P407 gel were found to have the same gelation temperature (Table 11). As observed, the presence of the BSA-PTX NPs did not influence the gelation temperature. Thus, it exhibited the same gelation temperature effect as the 18% P407 gel.

Table 11. Effect of BSA-PTX NPs s on $T_{sol\text{-}gel}$ (n = 3).

	18% P407/˚C	18% P407/2.5 mg/ml BSA-PTX NPs/˚C
$T_{sol\text{-}gel}$	30.1 ± 0.1*	30.1 ± 0.1*

3.10. *In Vitro* Drug Release

The *in vitro* drug release was investigated using two suitable dissolution media. The dissolution rate of PTX in the buffer at pH 5.5 was higher between 2 h and 24 h compared with that in the buffer at pH 7.4 (Figure 4).

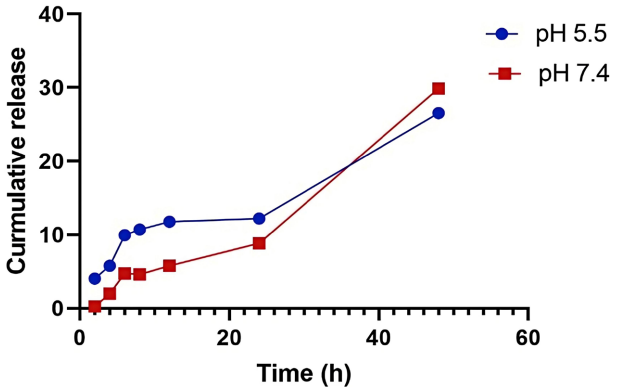

Figure 4. *In vitro* drug release of PTX from BSA-PTX NPs-loaded Gel.

4. Conclusion

The overall aim of this work was to prepare and evaluate the paclitaxel (PTX) loaded albumin nanoparticle formulated with thermosensitive hydrogel. In this study, we successfully prepared BSA-NPs (100 nm), loaded with PTX using the desolvation method and formulated into a thermo-sensitive hydrogel. Various factors such as BSA concentration, drug ratio, cross-linking agents, ethanol flow rate, and pH have profound effects on the size of nanoparticles, PDI, and drug encapsulation efficiency. The prepared nanoparticle exhibited high PTX encapsulation and good *in vitro* dissolution behavior. The synthesized PTX-loaded BSA-NPs thermosensitive hydrogel had a $T_{sol\text{-}gel}$ of 31.7 ± 0.1˚C, close to the target nasal temperature of 32˚C. From the various tests performed, two optimized formulations were observed; 19% P407/0.2% P188/0.5% HA and 20% P407/0.8% P188/0.5% HA. The two optimized formulations were characterized as follows: 1) 19% P407/0.2% P188/0.5% HA, with a phase transition temperature of 31.7 ± 0.1˚C and viscosity of 648.1 ± 16.6 mPa·s; 2) 20% P407/0.8% P188/0.5% HA, with a phase transition temperature of 31.5 ± 0.1˚C and viscosity of 777.3 ± 49.8 mPa·s. The first formulation is preferred for intranasal application due to its closer phase transition temperature to the target nasal temperature (32˚C) and moderate viscosity, which balances injectability and retention in the nasal cavity.

Conflicts of Interest

The authors declare no conflicts of interest regarding the publication of this paper.

References

[1] Khanna, C., Rosenberg, M. and Vail, D.M. (2015) A Review of Paclitaxel and Novel Formulations Including Those Suitable for Use in Dogs. *Journal of Veterinary Internal Medicine*, **29**, 1006-1012. https://doi.org/10.1111/jvim.12596

[2] Guchelaar, H., Ten Napel, C.H.H., de Vries, E.G.E. and Mulder, N.H. (1994) Clinical, Toxicological and Pharmaceutical Aspects of the Antineoplastic Drug Taxol: A Review. *Clinical Oncology*, **6**, 40-48. https://doi.org/10.1016/s0936-6555(05)80367-x

[3] Elsadek, B. and Kratz, F. (2012) Impact of Albumin on Drug Delivery—New Applications on the Horizon. *Journal of Controlled Release*, **157**, 4-28.

https://doi.org/10.1016/j.jconrel.2011.09.069

[4] Kratz, F. (2008) Albumin as a Drug Carrier: Design of Prodrugs, Drug Conjugates and Nanoparticles. *Journal of Controlled Release*, **132**, 171-183. https://doi.org/10.1016/j.jconrel.2008.05.010

[5] Elzoghby, A.O., Samy, W.M. and Elgindy, N.A. (2012) Albumin-Based Nanoparticles as Potential Controlled Release Drug Delivery Systems. *Journal of Controlled Release*, **157**, 168-182. https://doi.org/10.1016/j.jconrel.2011.07.031

[6] Hawkins, M.J., Soon-Shiong, P. and Desai, N. (2008) Protein Nanoparticles as Drug Carriers in Clinical Medicine. *Advanced Drug Delivery Reviews*, **60**, 876-885. https://doi.org/10.1016/j.addr.2007.08.044

[7] Desai, N. (2015) Nanoparticle Albumin-Bound Anticancer Agents. In: Crommelin, D. and de Vlieger, J., Eds., *Non-Biological Complex Drugs*, Springer, 335-354. https://doi.org/10.1007/978-3-319-16241-6_10

[8] Elzoghby, A.O., Samy, W.M. and Elgindy, N.A. (2012) Protein-Based Nanocarriers as Promising Drug and Gene Delivery Systems. *Journal of Controlled Release*, **161**, 38-49. https://doi.org/10.1016/j.jconrel.2012.04.036

[9] Destruel, P., Zeng, N., Maury, M., Mignet, N. and Boudy, V. (2017) *In Vitro* and *in Vivo* Evaluation of *in Situ* Gelling Systems for Sustained Topical Ophthalmic Delivery: State of the Art and Beyond. *Drug Discovery Today*, **22**, 638-651. https://doi.org/10.1016/j.drudis.2016.12.008

[10] He, C., Kim, S.W. and Lee, D.S. (2008) *In Situ* Gelling Stimuli-Sensitive Block Copolymer Hydrogels for Drug Delivery. *Journal of Controlled Release*, **127**, 189-207. https://doi.org/10.1016/j.jconrel.2008.01.005

[11] Radivojša, M., Grabnar, I. and Ahlin Grabnar, P. (2013) Thermoreversible *in Situ* Gelling Poloxamer-Based Systems with Chitosan Nanocomplexes for Prolonged Subcutaneous Delivery of Heparin: Design and *in Vitro* Evaluation. *European Journal of Pharmaceutical Sciences*, **50**, 93-101. https://doi.org/10.1016/j.ejps.2013.03.002

[12] Marwah, H., Garg, T., Rath, G. and Goyal, A.K. (2016) Development of Transferosomal Gel for Trans-Dermal Delivery of Insulin Using Iodine Complex. *Drug Delivery*, **23**, 1636-1644. https://doi.org/10.3109/10717544.2016.1155243

[13] Ur-Rehman, T., Tavelin, S. and Gröbner, G. (2011) Chitosan *in Situ* Gelation for Improved Drug Loading and Retention in Poloxamer 407 Gels. *International Journal of Pharmaceutics*, **409**, 19-29. https://doi.org/10.1016/j.ijpharm.2011.02.017

[14] Langer, K., Balthasar, S., Vogel, V., Dinauer, N., von Briesen, H. and Schubert, D. (2003) Optimization of the Preparation Process for Human Serum Albumin (HSA) Nanoparticles. *International Journal of Pharmaceutics*, **257**, 169-180. https://doi.org/10.1016/s0378-5173(03)00134-0

[15] Galisteo-González, F. and Molina-Bolívar, J.A. (2014) Systematic Study on the Preparation of BSA Nanoparticles. *Colloids and Surfaces B: Biointerfaces*, **123**, 286-292. https://doi.org/10.1016/j.colsurfb.2014.09.028

[16] Jun, J.Y., Nguyen, H.H., Paik, S., Chun, H.S., Kang, B. and Ko, S. (2011) Preparation of Size-Controlled Bovine Serum Albumin (BSA) Nanoparticles by a Modified Desolvation Method. *Food Chemistry*, **127**, 1892-1898. https://doi.org/10.1016/j.foodchem.2011.02.040

[17] Taheri, A., Dinarvand, R., Atyabi, F., Ahadi, F., Nouri, F.S., Ghahremani, M.H., *et al.* (2011) Enhanced Anti-Tumoral Activity of Methotrexate-Human Serum Albumin Conjugated Nanoparticles by Targeting with Luteinizing Hormone-Releasing Hormone (LHRH) Peptide. *International Journal of Molecular Sciences*, **12**, 4591-4608.

https://doi.org/10.3390/ijms12074591

[18] Kreuter, J. (2001) Nanoparticulate Systems for Brain Delivery of Drugs. *Advanced Drug Delivery Reviews*, **47**, 65-81. https://doi.org/10.1016/s0169-409x(00)00122-8

[19] Kakran, M., Sahoo, N.G., Tan, I. and Li, L. (2012) Preparation of Nanoparticles of Poorly Water-Soluble Antioxidant Curcumin by Antisolvent Precipitation Methods. *Journal of Nanoparticle Research*, **14**, Article No. 757. https://doi.org/10.1007/s11051-012-0757-0

[20] Dreis, S., Rothweiler, F., Michaelis, M., Cinatl, J., Kreuter, J. and Langer, K. (2007) Preparation, Characterisation and Maintenance of Drug Efficacy of Doxorubicin-Loaded Human Serum Albumin (HSA) Nanoparticles. *International Journal of Pharmaceutics*, **341**, 207-214. https://doi.org/10.1016/j.ijpharm.2007.03.036